Journal of Applied Polymer Science

Mechanical and thermal properties of biphenyldiol formaldehyde resin/gallic acid epoxy composites enhanced by graphene oxide

Shihui Chen,[1,2] Shufang Lv,[1] Guixiang Hou,[1] Li Huo,[1] Jungang Gao[1]
[1]College of Chemistry and Environmental Science, Hebei University, Baoding 071002, China
[2]Tangshan Sanyou Group Co., Ltd., Tangshan 063305, China
Correspondence to: J. Gao (E-mail: gaojg@mail.hbu.edu.cn) and L. Huo (E-mail: huolichenchen@sina.com)

ABSTRACT: In this study, the gallic acid-based epoxy resin (GA-ER) and alkali-catalysed biphenyl-4,4′-diol formaldehyde resin (BPFR) are synthesized. Glass fibre-reinforced GA-ER/BPFR composites are prepared. Graphene oxide (GO) is used to improve the mechanical and thermal properties of GA-ER/BPFR composites. Dynamic mechanical properties and thermal, mechanical, and electrical properties of the composites with different GO content are characterized. The results demonstrate that GO can enhance the mechanical and thermal properties of the composites. The glass transition temperature, T_g, of the BPFR/GA-ER/GO composites is 20.7°C higher than the pure resin system, and the 5% weight loss temperature, T_{d5}, is enhanced approximately 56.6°C. When the BPFR: GA-ER mass ratio is at 4 : 6 and GO content is 1.0–1.2 wt %, the tensile and impact strengths of composites are 60.97 MPa and 32.08 kJ/m^2 higher than the pure resin composites, respectively. BPFR/GA-ER composites have better mechanical properties, and can replace common BPA epoxy resins in the fabrication of composites. © 2015 Wiley Periodicals, Inc. J. Appl. Polym. Sci. **2015**, *132*, 42637.

KEYWORDS: composites; grapheme and fullerenes; mechanical properties; nanostructured polymers; nanotubes; thermosets

Received 9 January 2015; accepted 18 June 2015
DOI: 10.1002/app.42637

INTRODUCTION

Epoxy resins are high performance thermosetting polymers that have excellent adhesive properties, corrosion resistance, and high mechanical strength. Therefore, they are utilized extensively as adhesives, construction materials, laminates, and coatings. At present, most epoxy resins are industrially manufactured from bisphenol A (BPA).[1] The epoxy resin with the aromatic ring of BPA is particularly preferred in application since it has good thermal resistance. However, BPA is a hormonally active agent and exhibits an oestrogen-like property that can cause a disorder of human endocrine, such as the precocious puberty.[2,3] Therefore, some new types of epoxy resins without BPA are required for human health and environmental protection.

Because of depleting petrochemical reserves and rising environmental protective awareness, it is of the utmost importance to develop renewable resources that can replace petrochemical products. The emergence of renewable materials has opened up a different path to reduce the dependence on petrochemical resources. Materials derived from starch, cellulose, vegetable oil, and other natural polymers are attracting huge interest.[4,5]

The polyphenols, which can be obtained from renewable materials, is a potential resource which could provide thermal resistance epoxy resin with comparable mechanical properties to basic BPA.[6] Gallic acid (GA) is one of the polyphenols and can be obtained by hydrolyzing naturally occurring gallotannic acid, which is used as an anticancer agent and is abundant in nature. Recent papers have reported a fabrication method for gallic acid-based epoxy resins (GA-ER) that utilise the reaction of gallic acid with epichlorohydrin.[7,8]

As a two-dimensional one-atom-thick material, graphene has attracted tremendous attention since it was discovered in 2004. Graphene has extraordinarily high values of Young's modulus, thermal conductivity, charge carrier mobility, specific surface area, and has relatively low cost compared to carbon nanotubes (CNTs).[9,10] However, because of the van der Waals interactions between graphene sheets, it is easy for the sheets to aggregation, and therefore, it is difficult to achieve well dispersion in a polymer matrix.[11] Graphene oxides (GO), obtained by the exfoliation of graphite oxide, have a folded rough surface and a large number of epoxy and hydroxyl groups attached to the surface, as well as carbonyl and carboxyl groups attached to the edge of the sheet. In contrast to graphene, GO has excellent mechanical properties and solubility.[12] In addition, GO has favourable compatibility with polymers and the unique properties resulting from the incorporation of graphene and GO into polymers. GO has a wide range of potential applications, for example, a new type of filler for preparing high performance polymeric composites.[13–15] Bora *et al.* has reported the preparation of polyester resin/graphene oxide nanocomposite with improved mechanical

properties. Recent investigations have shown that GO can greatly improve the flexibility, flame resistance, and thermal stability of phenol and epoxy composites.[16–18] King *et al.* also reported mechanical properties of graphene nanoplatelet/epoxy composites.[19]

Phenol-formaldehyde resin (PFR) is part of the commonly used thermosetting resins owing to its excellent mechanical properties, and flame retardant and heat resistant property. PFR is utilized to prepare reinforced composites, insulation materials, adhesives, and most notably, aerospace materials. PFR can also be used as a curing agent for epoxy resins, which can improve the thermal properties of the epoxy resin, including the glass transition temperature (T_g) and thermal decomposition temperature.[20–22] By changing the ratio of phenol and formaldehyde and using different catalysts, the phenolic resins with different structures and properties can be achieved. Due to the intensive aromatic ring in biphenyl-4,4′-diol, the biphenyl-4,4′-diol is expected to result in a biphenyl-4,4′-diol formaldehyde resin (BPFR) with improved heat resistance and residual rates at elevated temperatures compared to PFR.

However, to the best of our knowledge, there has not been any study on BPFR-cured GA-ER and BPFR/GA-ER/GO reinforced composites. In this study, GO was utilized to modify the properties of glass fibre-reinforced BPFR/GA-ER composites, with the effect of GO on the mechanical, thermal, and dielectric properties of the composites investigated.

EXPERIMENTAL

Reagents and Materials

Gallic acid (GA), formaldehyde, ethanol, sodium hydroxide, sulfuric acid, epichlorohydrin, tetrabutylammonium bromide, potassium hypermanganate, hydrogen peroxide, *N,N*-dimethyl benzylamine, *N,N*-dimethylformamide (DMF) are all analytical reagents and supplied by Tianjin Kermel Chemical Reagent Co. China. Graphite powder (NG), purity > 99.95%, which have an average length about 45 μm, supplied by Qingdao golden day graphite, China. Biphenyl-4,4′-diol, chemical reagent, recrystallization at the 70°C in 30% aqueous solution of DMF, T_m 284°C. Bisphenol A epoxy resin (BPA-ER, type E-44), epoxy value: 0.44 mol/100 g, supplied by Wuxi Resin Factory, China. The vertically interwoven single layer glass fiber cloth with the thickness of 0.2 mm and the density of 230 g/m^2 is supplied by Guangzhou Vertrotex Chemical Materials Co. of China.

Synthesis of BPFR

BPFR was synthesized by the condensation reaction of biphenyl-4,4′-diol and formaldehyde in a molar ratio of 1 : 2.5, with the slow addition of sodium hydroxide (2.5 wt % of the total mass of the system). The reaction system was heated at 85°C for 120 min, followed by dehydration under vacuum conditions. Finally, a transparent viscous liquid was obtained, which had the chemical structure shown in Scheme 1(a). Gel permeation chromatography (GPC, BI2010, Brookhaven) was used to determine the various molecular weights of the synthesized BPFR. The number average molecular weight (M_n), weight average molecular weight (M_w), and molecular weight distribution (MWD) was determined to be 490, 655, and 2.67, respectively. The synthesized resin was then dissolved in ethanol to obtain an ethanol solution with 60 wt % BPFR. The molecule structure of BPFR is as Scheme 1 (a).

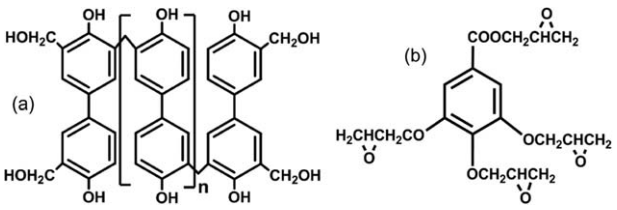

Scheme 1. Molecular structure of BPFR (a) and GA-ER (b).

Synthesis of GA-ER

GA-ER was prepared according to the methods reported in the literature.[7,23] Typically, 0.1 mol of GA, 2.0 mol of epichlorohydrin, and tetrabutylammonium bromide (3% of the molar ratio of GA) were added into a 500 mL four-neck flask under stirring. The mixture was heated to 100°C and stirred for 6 h, and then cooled to room temperature. Whereafter, 0.4 mol of NaOH was gradually added into the mixture and stirred for 2 h under reflux. Then the mixture was washed to neutralise with deionized water, and the residual epichlorohydrin and water were removed under vacuum conditions. Finally, a pale yellow, translucent and viscous liquid named GA-ER was prepared. The epoxy value of the GA-ER was determined with the hydrochloric acid-acetone method, and the result was 0.87 mol/100 g. The molecular structure of the GA-ER was characterized by NMR (Avance III 600 MHz, Bruker Co. Switzerland) and FTIR (640-IR, Varian Co.).

Synthesis of GO

GO was prepared via the modified Hummers method.[24] Five grams of graphite and 120 mL of concentrated H_2SO_4 were uniformly mixed in an ice bath. Then, 20 g of $KMnO_4$ was gradually added to the mixture with continuous stirring while the temperature was kept below 10°C. After stirring for 30 min, the mixture was slowly heated to 35°C in a warm water bath and stirred for a further 2.5 h. Then, 250 mL of deionised water were carefully added to the paste while the temperature was kept below 95°C. The mixture was then heated to ~90°C for an additional 20 min. Subsequently, 35 mL of H_2O_2 was hereby added dropwise, during which the colour of the mixture changed from brown to bright yellow. Liquid was processed with hydrochloric acid and diluted with deionised water. The diluted solution was ultrasonicated for 1 h and placed to stand for 3 days. The precipitate was repeatedly washed with deionised water and centrifuged until neutral. Deep yellow solids were obtained by freeze-drying the centrifuged material. X-ray diffraction (XRD, D/MAX-2500, Rigaku Denki, Japan), atomic force microscopy (AFM, Agilent 5500, Agilent) and transmission electron microscopy (TEM, Tecnai G2 F20 S-TWIN) were used to characterize the structure of GO sheets. AFM samples were prepared by spin-coating from extremely diluted DMF solutions onto processed silicon wafer substrates at 1200 rpm. TEM was used at an acceleration voltage of 60–200 kV and a resolution of 0.24 nm.

Preparation and Characterization of the Nanocomposites

BPFR/GA-ER/GO nanocomposites were prepared as follows: first, some GO was dispersed in 4.0 g of the BPFR in ethanol, ultrasonicated for 1 h; then 6 g of GA-ER, 10 mL of acetone and 0.1 g of *N,N*′-dimethylbenzylamine (a catalyst) were added to the GO/BPFR solution, ultrasonicated for 1 h and the nanocomposite of BPFR/GA-ER/GO was prepared at last. Using the

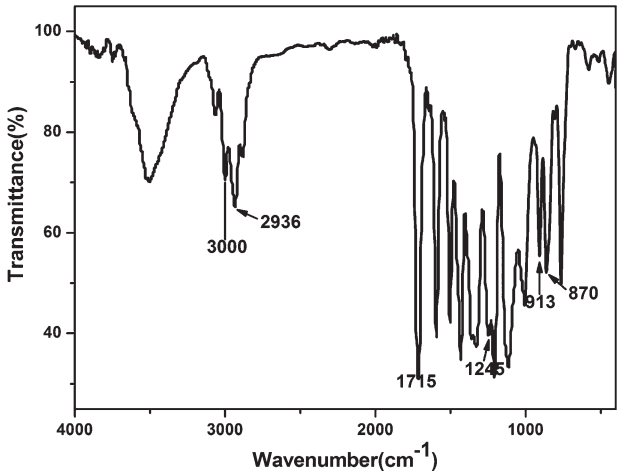

Figure 1. FT-IR spectrum of GA-ER.

same mass ratio of BPFR to GA-ER (4 : 6) and preparation method, a series of resins containing 0, 0.2, 0.3, 0.4, 0.6, 0.8, 0.9, 1.0, 1.2, 1.5, and 2.0 wt % of GO were prepared and named as No. 0, No. 2, No. 3, No. 4, No. 6, No. 8, No. 9, No. 10, No. 12, No. 15, and No. 20, respectively. The dispersion state of GO in the resin and its morphology were characterized with transmission electron microscopy (TEM, JEM-100SX, Electro Co. Japan).

The curing reaction process of the resins was tracked by Fourier transform infrared spectrometer (FTIR, FTS-40, BIO-RAD) with KBr tablet method. The sample was dissolved in acetone and then coated on the KBr tablet, then the acetone was volatilized under vacuum at room temperature; after that the sample was cured at 120°C for 0, 10, and 30 min, and the change of the spectra was determined by FTIR, respectively.

The thermal stability of the cured resins of BPFR/GA-ER/GO with varying GO content was performed on a thermogravimetric analyzer (TG, Pyris-6, Perkin-Elmer). The sample was heated from 25 to 850°C at a heating rate of 10°C/min in static air.

The laminates of BPFR/GA-ER/GO resin with glass fibre cloth were prepared by hot pressing method and the mass ratio of BPFR/GA-ER/GO resin to glass fiber cloth were controlled constant at 1 : 1 in different laminates. A heat-cleaned glass fiber cloth was coated with the resin solution, and the solvent only was removed under vacuum. Laminate was prepared with 5 pieces of resin-containing cloth and was cut into strips (25 × 5 × 1 mm) for dynamic mechanical analysis. In order to avoid bubbles in the laminate during the preparing process, the resin-containing glass fiber cloth was pre-cured into B stage at 120°C. Then the pre-cured samples were hot-pressed by a thermo-compressor. The thermo-compressor was operated with gradually increasing pressure at 160°C, and then cured at 200°C for 30 min under high pressure. The dynamic mechanical properties of the materials were characterized with a dynamic mechanical analyzer (DMA, DMA8000, Perkin-Elmer). The single-cantilever vibration mode was used and the sample was heated from −100 to 250°C at a heating rate of 2°C/min with the frequency of 2 Hz.

Three-mm-thick laminate of glass fibre-reinforced composites with different GO contents was prepared with 15 pieces of resin-containing cloth following the same method and conditions as described above in DMA testing samples. The laminates were cut into strips (100 × 10 × 3 mm) for to determine the tensile and impact strengths according to the ASTM D 3039 and D256, respectively. The tensile tests were performed on an electronic tensile tester (WSM-20kN, Changchun Equipment, China) at an extension rate of 10.0 mm/min, and at 25°C and 50% relative humidity. The notch impact test (the depth of the V notch was 1 mm) was carried on a XCJ-40 impact tester. The morphology of the fractured surfaces of the laminate was characterized with scanning electron microscopy (SEM, JSM-7500F, Electro Co. Japan).

The electrical properties were determined by high-frequency Q meter, (QBG-3D type, Shanghai Ai Yi Electronic Equipment, China). The resonance method was used to determine the capacitance of the 3 mm laminates, the inductance value of the inductance coil is L = 1 mH, $C_0 \approx 8$ pF, the frequency of the first resonance is between 1.8 and 5 MHz.

To compare with bisphenol-A epoxy resin (BPA-ER, type E-44), under the same condition, the glass fiber reinforced laminate of BPFR/BPA-ER was prepared and the mechanical properties were determined.

RESULTS AND DISCUSSION

Chemical Structure Analysis of the GA-ER

The GA-ER product obtained from the gallic acid was analyzed by FT-IR. Figure 1 shows the FT-IR spectrum of GA-ER. In Figure 1, the absorption peaks at 3000 and 870 cm^{-1} were associated with the C–H vibration absorption belong to the benzene ring skeleton. Absorption peaks at 2936 cm^{-1} was attributed to vibration of the CH_2 cm^{-1} in the GA-ER molecule. The absorption peak at 913 cm^{-1} was attributed to vibration of the epoxy groups. The absorption peak at 1715 cm^{-1} was associated with the C=O vibration of the ester carbonyl. The absorption peak at 1245 cm^{-1} was attributed to vibration of the –O–CH_2–.

Figure 2 is the ^{1}HNMR spectrum of GA-ER. ^{1}HNMR (C_3D_6O, δppm): 7.35–7.5 (m, 2H, benzene ring), 4.2–4.73 (m, 8H, methylene), 3.29–3.52 (m, 4H, epoxy group), 2.66–2.87(m, 8H, epoxy group). The results show that the gallic acid epoxy resin (GA-ER) had been synthesized, and the molecule structure of GA-ER is as follows Scheme 1 (b).

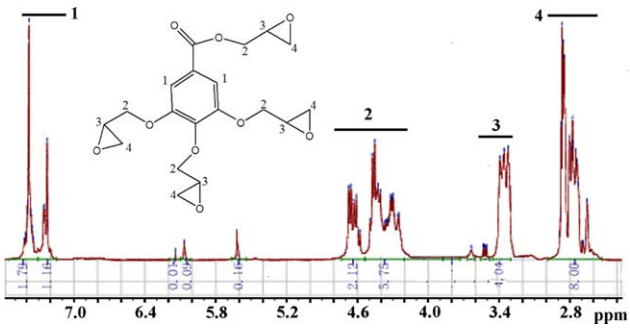

Figure 2. ^{1}HNMR spectrum of GA-ER. [Color figure can be viewed in the online issue, which is available at wileyonlinelibrary.com.]

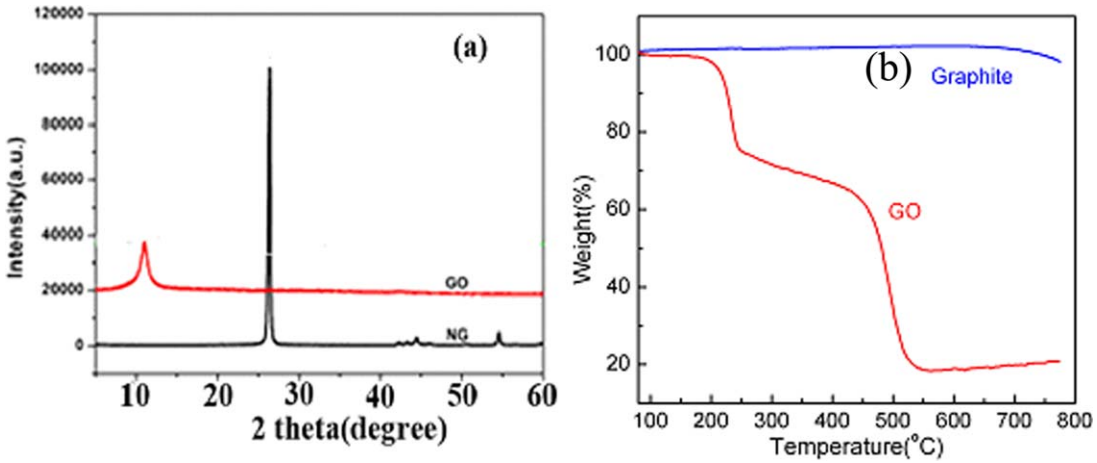

Figure 3. XRD pattern and TG curves of GO and NG. [Color figure can be viewed in the online issue, which is available at wileyonlinelibrary.com.]

Analysis of GO Structure

Figure 3 shows the X-ray diffraction pattern and thermal weight loss of GO and NG. The little diffraction peak at $2\theta = 10.6°$ corresponds to the characteristic (001) crystal face of GO, with an interplanar spacing of 8.35 Å, the high characteristic diffraction peak at $2\theta = 26°$ corresponds to graphite. Figure 3(b) shows that the natural graphite (NG) has only a little weight loss before 550°C, but the GO has obvious heat weight loss at about 200°C, this attributes to the thermal decomposition of oxygen-containing groups on the graphene surface, because they have a low decomposition temperature.

Figure 4(a) shows the AFM images of GO. As can be seen, the GO has a lamellar structure and the average thickness is about 1.2 nm, which is probably caused by the stacking of individual layers. It shows that the oxygen-containing functional groups were inserted into the lamellar structure of graphite in the presence of the strong oxidizing agent, which increased the interlayer spacing. After a further ultrasonic treatment, multilamellar GO was exfoliated to produce single layer GO. Figure 4(b) is the TEM images of GO, it shows that the GO has a folded sheet structure with a rough surface.

Curing Analysis of BPFR/GA-ER

Figure 5 is the FT-IR spectra of BPFR/GA-ER system curing for a different time at 120°C. It can be seen an obvious absorption peak at 913 cm^{-1} in the spectra for the uncured sample (a). However, after curing at 120°C in the presence of *N,N′*-dimethylbenzylamine, the epoxy absorption peak at 913 cm^{-1}gradually decreased with the increasing curing time, and this characteristic peak finally disappeared after curing for 30 min, the it indicates the curing reaction of epoxy group has completed.

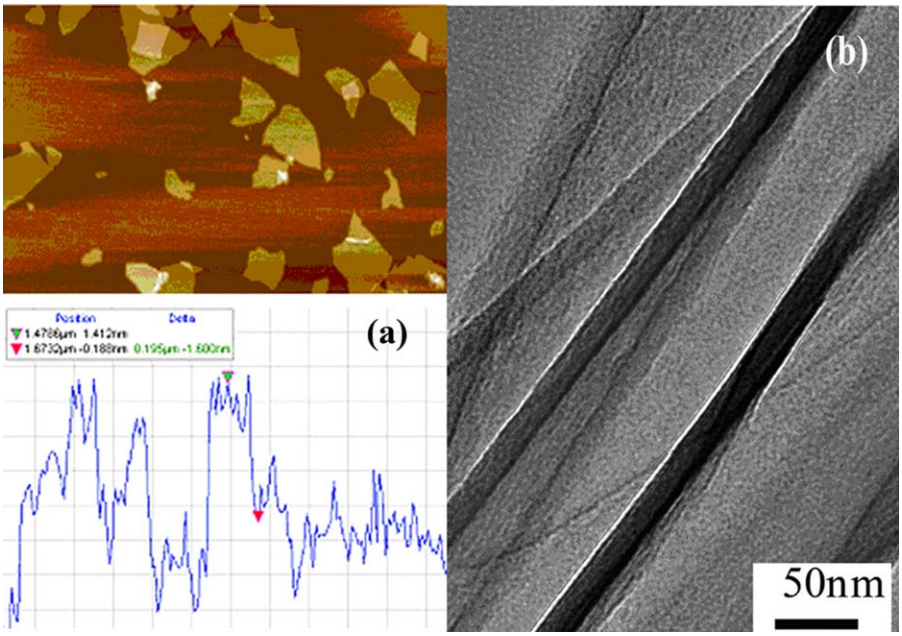

Figure 4. AFM and TEM image of GO. [Color figure can be viewed in the online issue, which is available at wileyonlinelibrary.com.]

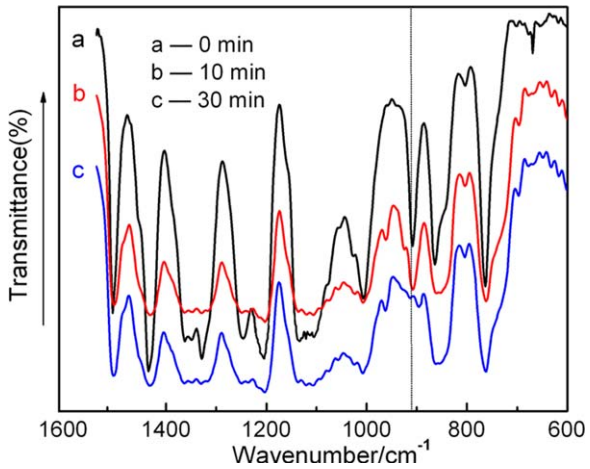

Figure 5. Curing FT-IR spectra of BPFR/GA-ER with different time at 120°C. [Color figure can be viewed in the online issue, which is available at wileyonlinelibrary.com.]

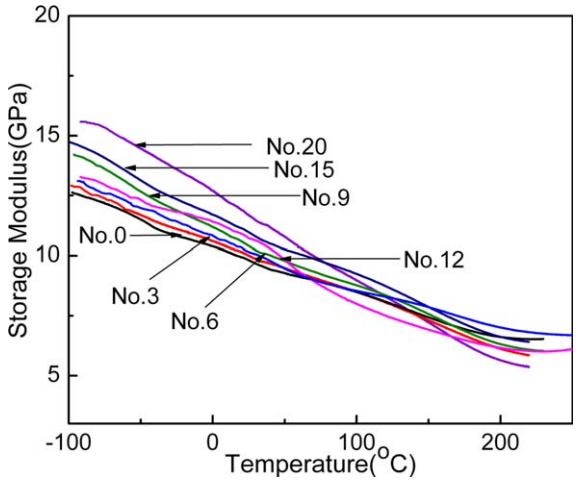

Figure 6. DMA storage modulus curves of BPFR/GA-ER/GO composites with different GO contents. [Color figure can be viewed in the online issue, which is available at wileyonlinelibrary.com.]

Dynamic Mechanical Analysis (DMA) of the Cured Samples

Polymers are typical viscoelastic materials, and the performance is essentially a reflection of their molecular motion and physical state. When alternating stress is applied to a polymer, part of the mechanical energy is used to change the conformation of the molecular chains, and the other part is stored as elastic potential energy. Meanwhile, the coiling or stretching of molecular chains is needed to overcome the friction between molecules, with the energy lost converted into heat. The storage modulus E' reveals the amount of elastic energy saved in a material and its rigidity. Figure 6 shows how the storage modulus changes as a function of both the temperature and GO content. As can be seen, the storage modulus for each sample decreases as the temperature increases from −100 to 200°C. This is related to the more aromatic group in the molecular chain and the four epoxy groups are all connected to the same aromatic ring, which affects the packing density of the molecular chain and has more free volume in the materials. The storage modulus of the samples increases with increasing GO content. This can be assigned to the characteristic structure of GO. The oxygen-containing group on the surface and edge of GO sheets can react with BPFR and GA-ER, and the rough surface of GO sheets may help it adsorb macromolecular segments. Zhu and Pignatello have reported that π–π interactions are the main mechanisms regulating the adsorption of both π-acceptors and π-donors onto the graphene surface.[25] Lin *et al.* reported the adsorption and suspending process of tannic acid on the surface of CNTs.[26] They proved that tannic acid molecules were adsorbed onto CNTs by the acid's aromatic rings binding to the surface carbon rings via π-π interactions, until forming a monolayer.[26] These reactions with GO and the adsorption of GO will restrict the motion of molecular segments and increase the rigidity of the material.

However, when the content of GO is over 1.5 wt %, the storage modulus decreases contrarily at high temperature. This is because excessive amounts of the GO will cause the aggregation, and therefore, decreases the rigidity and storage modulus of the material. The sample with GO content of 1.5 wt % has the highest storage modulus at high temperatures, which indicate that this composite has the optimum rigidity.

Figure 7 shows the mechanical loss (tanδ) spectra of the BPFR/GA-ER composites with different GO contents. As can be seen, all of the samples have a β peak at about −70 to −50°C. This corresponds to the secondary relaxation movement of the ether-containing chain segments, which enhances the toughness of the materials at low temperatures. It is also related to why the storage modulus decreases with increasing temperature. According to the relationship between the molecular motion of a polymer and temperature, the glass transition corresponds to the change from froze to move macromolecular chain segments. The tanδ value is the ratio of the loss modulus to storage modulus. DMA can be used to determine the temperature of the maximum tanδ peak (T_p) of the polymers. The one-to-one relationship between T_g and T_p means that the T_p is often

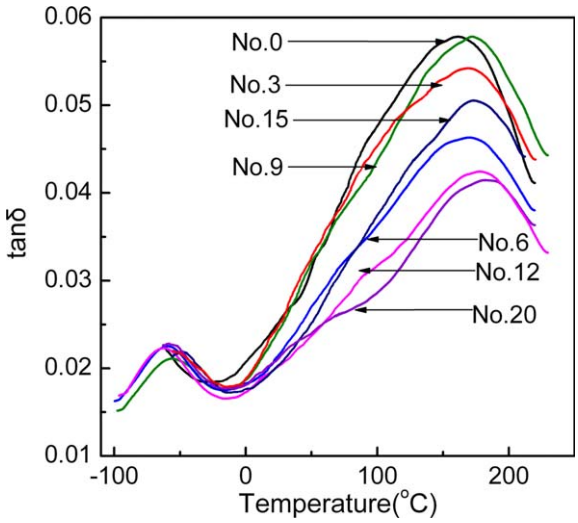

Figure 7. DMA tanδ spectra of BPFR/GA-ER with different GO contents. [Color figure can be viewed in the online issue, which is available at wileyonlinelibrary.com.]

Table I. T_g and Crosslink Density V_e of the BPFR/GA-ER Composites with Different GO Contents

Samples	No. 0	No. 3	No. 6	No. 9	No. 12	No. 15	No. 20
T_g(°C)	161.6	168.8	169.9	171.5	175.8	177.4	182.4
V_e (mol/m^3)	2.66×10^6	2.69×10^6	2.79×10^6	2.76×10^6	2.65×10^6	2.69×10^6	2.17×10^6

designated as T_g.[27,28] The higher T_p is, the higher the value of T_g. The tanδ α peak temperatures, T_g, for samples with increasing GO content are listed in Table I. It shows that T_g increases with increasing GO content correspondingly. Compared to the No. 0 pure resin sample, the T_g of the No. 20 composite has increased from 161.6°C to 182.4°C. This is because GO has a large specific surface area and a folded, rough, two-dimensional structure, and as a result, the contact area and adsorption between the GO and resin matrix increases with increasing GO content.[25,26] The carboxyl and hydroxyl groups on the surface of a GO layer can also react with the resin molecules. This will greatly limit the motion of the molecular segments, extending the relaxation process, and thus, resulting in a high transition temperature.[29]

In general, the crosslink density and chemical structure of the epoxy and curing agents have an important role in the T_g and thermal stability of the polymeric materials. The average crosslink density V_e of the cured composites could be estimated by the rubbery plateau modulus in DMA.[30,31] According to literature 31, we have:

$$V_e = E'/(6RT) \tag{1}$$

where V_e is crosslink density (mol/m^3); E' is the storage modulus estimated by DMA at the $T = T_g + 40$; R is gas constant (8.31446 J/K/mol).

Table I shows also the average crosslink density (V_e) of the BPFR/GA-ER/GO composites estimated from the storage modulus of DMA spectra. As can be seen from the data, V_e increases with increasing GO content correspondingly, except individual point error caused by sample size difference (No. 3). When the content of GO is 0.6–0.9 wt %, the V_e has maximum value, exceeds 0.9 wt % (No. 9), V_e decreased. It illustrates that GO has good distribution in the resin with appropriate contents and can form more crosslinking point between resin and GO. But exceeding this content, the crosslinking density decrease, which attributes to the aggregation of excessive amounts of GO. This phenomenon is different with T_g, because T_g is affected by a number of factors.

Thermal Degradation Behavior of the Composites

The thermal degradation behaviours and kinetics of polymer-based materials often follow complex mechanisms, and therefore, elucidating the kinetics for every step is very demanding. The thermal degradation of materials is considered in order to ascertain the processing parameters and appropriate working conditions of the materials, and thus, the use of simple empirical models in kinetic analysis is justified. Generally, some methods based on certain models and simplified designs are used to investigate the thermal degradation kinetics of polymers. Since thermal degradation is a multifaceted process, it is generally supposed that the system is under adiabatic conditions. If t is the reaction time and α is the degree of conversion, then the rate of weight loss is given by dα/dt, where the rate constant, k, and function of the concentration of reactants, $f(\alpha)$, have the following relationship.[32–34]

$$d\alpha/dt = k \cdot f(\alpha) \tag{2}$$

In the case of polymer degradation, it is usually supposed that the rate of conversion is proportional to the concentration of reactants that has not reacted yet; therefore,

$$f(\alpha) = (1-\alpha)^n \tag{3}$$

According to the Arrhenius equation and combining eqs. (2) and (3), the following eq. (4) can be obtained:

$$\frac{d\alpha}{dt} = A(1-\alpha)^n \exp\left(-\frac{E_a}{RT}\right) \tag{3}$$

where E_a is apparent activation energy (kJ/mol); A is a preexponential factor (min^{-1}); n is the apparent order of reaction; R is gas constant (8.31446 J/K/mol); T is Kelvin (K), respectively.

When the heating rate β is constant, $\beta = dT/dt$, the above eq. (4) can be changed into eq. (5):

$$\frac{d\alpha}{dT} = \frac{A}{\beta}(1-\alpha)^n \exp\left(-\frac{E_a}{RT}\right) \tag{4}$$

According to eq. (5), using different mathematical processing methods, we can get dynamics calculation method of the different thermal degradation. In this work, the Friedman method was used to derive kinetic parameters from TG data.[35]

Taking the logarithm of both sides of the eq. (4), we get the following eq. (6):

$$\ln\left(\frac{d\alpha}{dt}\right) = \ln\left(\beta \cdot \frac{d\alpha}{dT}\right) = \ln A + n\ln(1-\alpha) - \frac{E_a}{RT} \tag{6}$$

When the thermal loss rate dα/dt is constant, ln$A$ and $n$ln(1–α) is a constant, plotted ln(dα/dt) $\sim$ 1/T is a straight line. E_a of different thermal weight loss rate can be calculated from the slope of the line. As for ln(1$-\alpha$) $\sim$ 1/T, reaction order n can be obtained.[29,34]

The thermal stability of the material can be identified with three temperature parameters: T_{d5}, the temperature corresponding to 5% weight loss; T_{md}, the temperature corresponding to the loss of 50 wt %, and the residual rate at 800°C. Table II shows the various temperature parameters for the samples. Figure 8 shows the thermogravimetric (TG) curves of the samples with different GO contents.

As can be seen from Figure 8 and Table II, the characteristic temperatures of the samples increase with increasing GO content at a heating rate of 10°C/min, and the thermal residual rate at 800°C increases significantly. Both of these factors illustrate that the thermal stability of the composites is enhanced by the addition of GO. Notably, compared to the No. 0 pure resin

Table II. Temperature Parameters of TG Curves for BPFR/GA-ER/GO Composites with Different GO Contents

Samples	T_{d5}/°C	T_{md}/°C	Residual wt %
No. 0	198.3	460.2	9.24
No. 2	229.8	498.4	10.13
No. 4	254.9	496.8	17.46
No. 6	246.6	517.9	24.53
No. 8	250.9	502.7	25.59
No. 10	248.6	519.1	27.42
No. 12	248.2	531.5	29.01
No. 15	206.3	533.1	34.35
No. 20	235.3	514.4	33.24

sample, the T_{d5} of the No. 4 composite has increased from 198.3°C to 254.9°C, which is 56.6°C higher than No. 0. This results from the fact that the lamellar structure of the GO can reduce the diffusion of volatile components in the material. On the other hand, the oxygen-containing functional groups on the surfaces and edges of GO sheets can react with BPFR and GA-ER, and which will increases the crosslink density of the materials as shown in Table I and also restricts the movement of the molecules, and decreases the diffusion of volatile components. These factors will all enhance the T_{d5} values.[36] Furthermore, GO does not have ordered crystal form compared to graphite, and thus, it has poor thermal conductivity. Therefore, when GO is uniformly dispersed in the composite, it will form a barrier that reduces thermal conduction and gas diffusion.[37] In addition, the π bond of GO on the surface can also absorb free radicals formed by thermal degradation and terminate free radical chain degradation reactions, which will also postpone the thermal degradation of the resin.

In order to investigate the thermal degradation activation energy, E_a, and reaction order n of the degradation process, the No. 0 and No. 12 samples were used only for analysis. The thermal degradation was determined at heating rates of 5, 10, 15, 20, and 25°C/min. The TG curves for the No. 0 and No. 12 samples are shown in Figure 9.

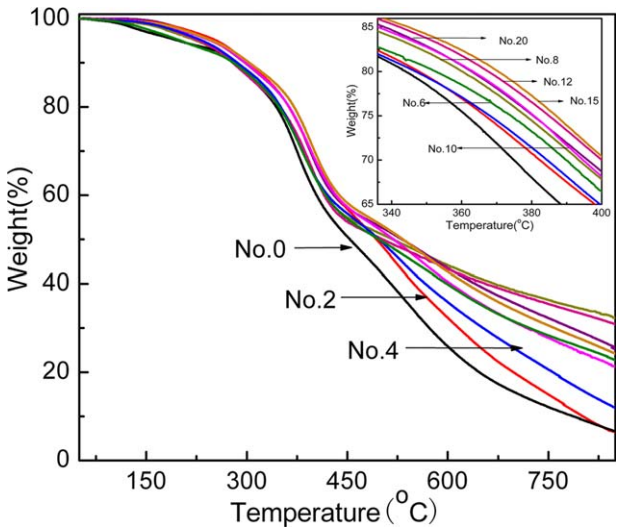

Figure 8. TG curves of BPFR/GA-ER composites with different GO contents. [Color figure can be viewed in the online issue, which is available at wileyonlinelibrary.com.]

According to the derivative curves of the samples for different heating rates, the thermal degradation process of the composites is roughly classified into three stages. The first stage is between 150 and 300°C, where the weight loss is about 5 wt %, which is caused by the evaporation of moisture and other small molecules. The second stage is between 300 and 500°C, the weight loss at this stage is mainly caused by the oxidative cleavage of ether bonds, carbonyl groups, and C–H bonds, with the maximum weight loss rate occurring at 430°C. As the temperature of the samples reaches 480°C, the weight loss of the composites is almost 50 wt %. Therefore, the extensive thermal degradation during the second stage means it can be examined the

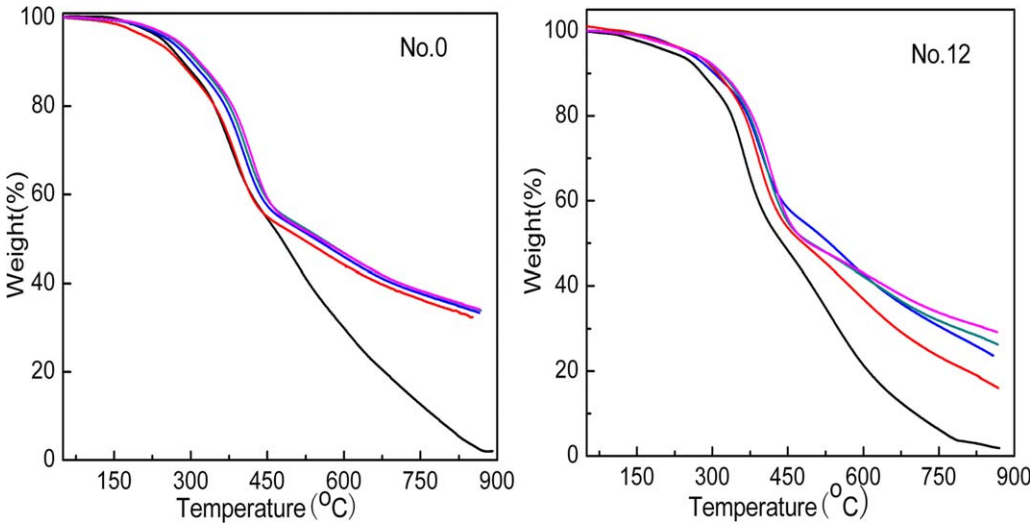

Figure 9. TG curves of No. 0 and No. 12 at different heating rates. [Color figure can be viewed in the online issue, which is available at wileyonlinelibrary.com.]

Table III. Thermal Degradation Kinetic Parameters of No. 0 and No. 12 by Friedman Method

Samples	β (°C/min)	E_a/kJ/mol	r_1	n	r_2
No. 0	5	25.43	−0.9971	1.84	0.9954
	10	22.87	−0.9937	1.68	0.9928
	15	24.76	−0.9941	1.82	0.9909
	20	26.89	−0.9933	1.94	0.9904
	25	26.42	−0.9919	1.79	0.9887
	Mean	25.27	-	1.82	-
No. 12	5	30.87	−0.9911	1.83	0.9969
	10	27.29	−0.9907	1.96	0.9925
	15	29.10	−0.9899	1.96	0.9894
	20	29.71	−0.9891	1.89	0.9879
	25	29.63	−0.9867	1.82	0.9884
	Mean	29.32	-	1.89	-

dominant stage of thermal degradation. The third stage is between 500 and 650°C, where the degradation and oxidation of aromatic rings and carbonization of the resin occur. In this stage, the degradation process of resin is slow.

The thermal degradation kinetics of the second stage was investigated using the Friedman method with a dynamic treatment.[35] According to eq. (6), the average E_a for the different heating rates and α of each sample can be calculated from the plot of $\ln(d\alpha/dt)$ against $1/T$, and the reaction order, n, can be obtained from the plot of $\ln(1-\alpha)$ against $1/T$. The E_a and n for No. 0 and No. 12 are listed in Table III, the linear relative coefficients of E_a and n are all between 0.9879 and 0.9977.

As shown in Table III, the average E_a of the two samples calculated with the Friedman method are 25.27 kJ/mol (No. 0) and 29.32 kJ/mol (No. 12), while the calculated average n of these samples are 1.82 (No. 0) and 1.89 (No. 12). It also shows that

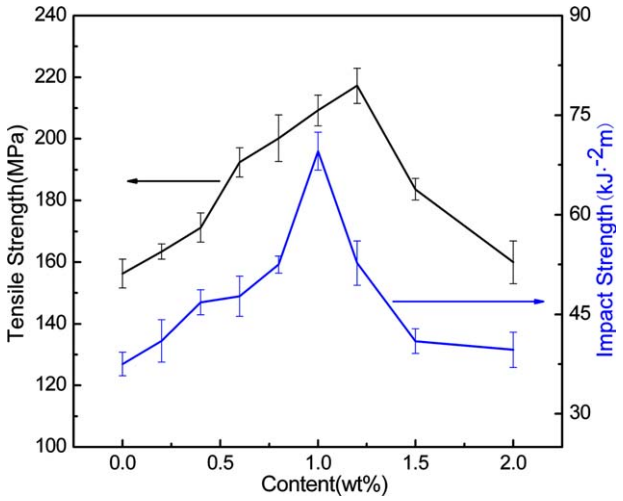

Figure 10. Mechanical strength of BPFR/GA-ER/GO laminates with different GO contents. [Color figure can be viewed in the online issue, which is available at wileyonlinelibrary.com.]

Table IV. Mechanical Strength of BPFR/GA-ER/GO Laminates with Different GO Mechanical Strength of BPFR/GA-ER/GO Laminates

Samples	Tensile Strength (MPa)	Standard deviation	Impact strength (kJ/m^2)	Standard deviation
No. 0	156.26	4.65	37.48	1.77
No. 2	163.48	2.46	40.97	3.18
No. 4	171.20	4.74	46.78	1.88
No. 6	192.41	4.75	47.70	3.01
No. 8	200.18	7.56	52.49	1.29
No. 10	209.24	4.97	69.56	2.85
No. 12	217.23	5.74	52.71	4.64
No. 15	183.64	3.53	40.93	1.85
No. 20	159.96	6.94	39.64	2.67

the GO-containing samples have higher thermal degradation E_a values than the pure resin system. This is coincides with the higher thermal degradation temperatures of the GO-containing samples as listed in Table II.

Mechanical and Electrical Properties of the Composites

According the mass ratio of resin and glass cloth was constant at 1 : 1, laminates were prepared for to test the mechanical properties. The mechanical properties of the composites as a function of GO content are shown in Figure 10 and Table IV (all points plotted are the average of the results of 5 samples). It can be observed that the tensile and impact strengths increase with increasing GO content. When GO content is 1.0–1.2 wt %, tensile strength is 217.23 MPa and the impact strength is 69.56 kJ/m^2, which is enhanced by 28.0% and 46.0%, respectively, compared to that of No. 0. This suggests that the mechanical properties of BPFR/GA-ER composites are improved by the addition of GO.

Figure 11 shows the SEM and TEM image of No. 10 BPFR/GA-ER/GO resins. As seen from Figure 11(a), the SEM image of sample No. 10 has rougher or blurred fractured surfaces. This indicates that some of the GO are pulled out from the resin matrix because of the impact stress, and as a result, produces cavities and craze, which absorbs part of the impact energy.[38,39] Figure 11(b) shows that the GO has a relatively uniform distribution. As previously described, the oxygen-containing functional groups on the surfaces and edges of GO sheets can react with BPFR and GA-ER, and increases the crosslink density of the materials as showed in Table I. These chemical and physical interactions between GO and the resin matrix restrict the movement and slippage of the polymer chains and increase the tensile strength of the composites. Individual GO layers have a very high mechanical strength and a rough surface.[40] Carbon atoms in a GO sheet are flexibly linked; when a force is applied to the sheet, it is able to adapt to the external force by bending itself rather than rearranging bonds. Therefore, this load transfer property increases the structural stability and impact strength.[23,41] Thus, the mechanical properties of the composites are all enhanced.

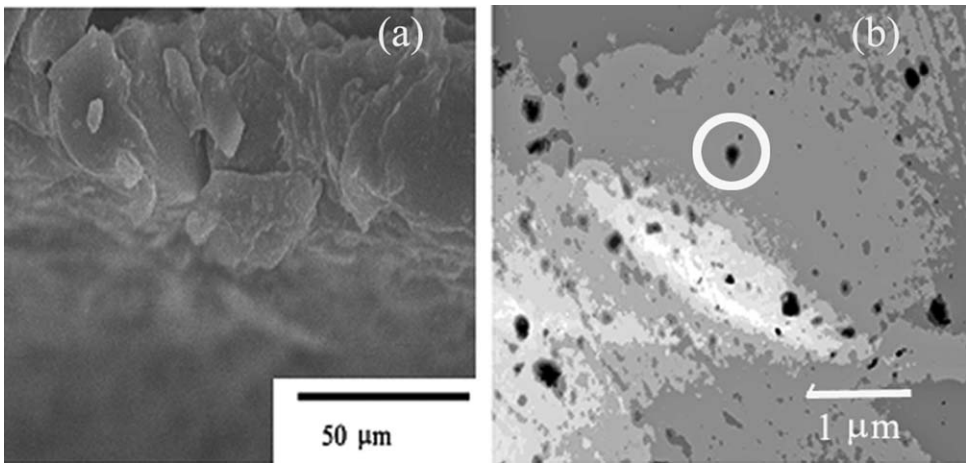

Figure 11. SEM and TEM image of No. 10 BPFR/GA-ER/GO resin.

However, the mechanical properties of the composites show a tendency to decrease slightly if they have high GO contents. This is from the fact that excessive amounts of GO cannot be evenly dispersed and can form aggregations in the composite. To a certain extent, this will lead to the formation of defects, and as a result, the composite can no longer effectively transfer loads.[42] In addition, the large amount of oxygen-containing groups on the GO will decompose in the material after the heating process over 160°C. Achaby had also observed that the various oxygen-containing groups on the GO would decompose between 150 and 210°C and had a maximum temperature of 195°C.[43] The generated gas from decomposition of oxygen-containing groups on GO would be produced micropores in the materials. As a consequence, the mechanical properties of the materials will be decreased.

To further investigate the effects of GO content on the reinforcement of the composites, SEM images of the fractured surfaces of No. 0 and No. 10 samples are shown in Figure 12. As can be seen, glass fibre-reinforced BPFR/GA-ER composites have good interfacial adhesion between glass fibres and resin. However, the differences between the SEM images of No. 0 and No. 10 are noticeable; the No. 0 interface between the resin and glass fibres is clear and the resin in sample No. 0 has a smoother fractured surface than No. 10. It shows that the No. 10 sample has stronger bonding with the glass fibres than that of No. 0. This is because some functional groups (hydroxyl and epoxy groups) on the surface of GO can also react with hydroxyl groups on the surface of the glass fibres, and therefore, enhance the bonding strength between the fibres and the resin matrix.

To compare the mechanical properties of GA-ER with common bisphenol A epoxy resin, glass fibre-reinforced composites of BPFR/E-44 (mass ratio of BPFR/E-44 is also 4/6) were prepared and tested according the same methods described above. The tensile and impact strengths of glass fibre-reinforced BPFR/E-44 composites are 112.35 MPa and 29.37 kJ/m^2, respectively, which are lower than that of No. 0 (156.26 MPa and 37.48 kJ/m^2, respectively). This shows that the BPFR/GA-ER composites have

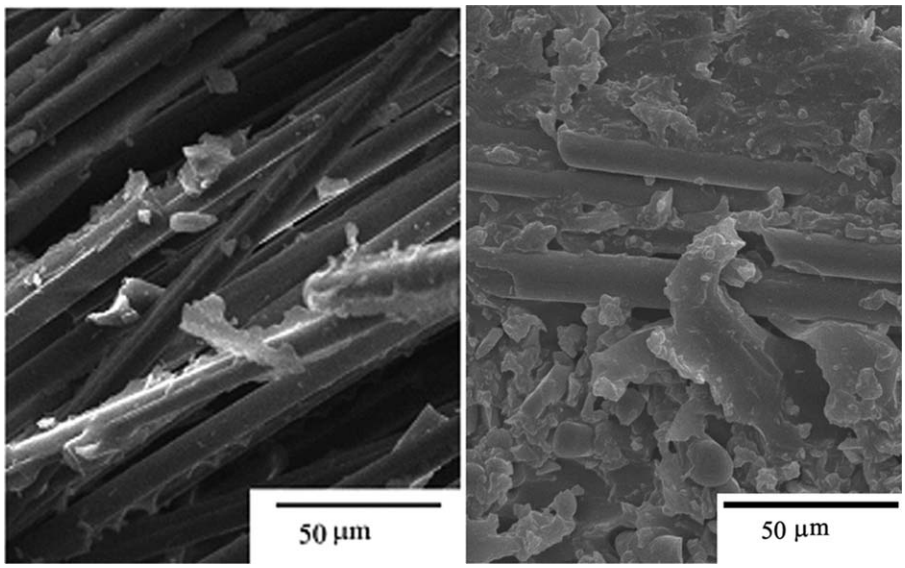

Figure 12. SEM images of impact breaking surface for No. 0 and No. 10.

Table V. Dielectrical Properties of BPFR/GA-ER/GO Composites with Different GO Contents

Samples	tanδ	ε
No. 0	0.0232	6.63
No. 2	0.0304	7.87
No. 4	0.0230	8.27
No. 6	0.0208	10.84
No. 8	0.0233	9.30
No. 10	0.0243	9.29
No. 12	0.0231	9.99
No. 15	0.0218	9.29
No. 20	0.0208	8.35

better mechanical properties, and GA-ER has the potential to replace common BPA epoxy resins in the fabrication of glass fibre-reinforced composites.

Table V illustrates how the electrical properties of the composites change with the addition of GO. These data show that after adding GO, the dielectric loss tanδ) does not change much, but the dielectric constant, ε, increases with increasing GO content. This is ascribed to the large amount of hydroxyl groups generated during the curing process that increases the polarity of the polymer chains, but the reaction and adsorption between the resin and GO hinder the movement of these polar groups when placed in an electric field. It is well known that the fabrication of GO destroys the conjugating structure of graphite, and as a result, GO has low electrical conductivity. Therefore, when GO is incorporated into a composite, the dielectric properties of the materials only change slightly. When compared to other polymer matrices, the BPFR/GA-ER/GO composite has a relatively higher dielectric constant and lower dielectric loss. That is to say, the BPFR/GA-ER/GO composites have improved dielectric properties, heat resistance, and ageing resistance, which are useful as electrically insulating materials and capacitor materials.

CONCLUSIONS

In this study, gallic acid-based epoxy resin (GA-ER) and alkali-catalysed biphenyl-4,4′-diol formaldehyde resin (BPFR) was utilized to prepare glass fibre-reinforced composites, and graphene oxide (GO) was used to improve the properties of composites. By these studying, the main conclusion as follows:

1. Exfoliated GO can be utilized to modify the properties of glass fibre-reinforced BPFR/GA-ER composites. The measured value of T_g for a BPFR/GA-ER/GO composite is ~22.7°C higher than the BPFR/GA-ER composite.
2. The addition of GO can increase the heat resistance of BPFR/GA-ER. Compared to the cured pure resin, the addition of GO can increase the 5 wt % loss temperature T_{d5} by 56.6°C.
3. The tensile and impact strengths of a BPFR/GA-ER/GO composite containing 1.0–1.2 wt % GO were 217.23 MPa and 69.56 kJ/m^2, which are increases of 28.0% and 46.0%, respectively, compared to that of the BPFR/GA-ER composite. BPFR/GA-ER composites have better mechanical properties than BPA-ER, and can replace common BPA epoxy resins in the fabrication of composites.

ACKNOWLEDGMENTS

The authors acknowledge the financial support from the Natural Science Foundation (No. E2015209264) and the High Level Talents Foundation (No. A201400504) of Hebei Province, China.

REFERENCES

1. Mohan, P. A. *Polym. Plast. Technol. Eng.* **2013**, *52*, 107.
2. Okada, H.; Tokunaga, T.; Liu, X.; Takayanagi, S.; Matsushima, A.; Shimohigashi, Y. *Environ. Health Persp.* **2008**, *116*, 32.
3. Flint, S.; Markle, T.; Thompson, S. *J. Environ. Manage.* **2012**, *104*, 19.
4. Mensah, B.; Kim, S.; Arepalli, S.; Nah, C. *J. Appl. Polym. Sci.* **2014**, *131*, 16, app 40640.
5. Auvergne, R.; Caillol, S.; David, G. *Chem. Rev.* **2014**, *114*, 082.
6. Hsu, S. H.; Chen, R. S.; Chang, Y. L.; Chen, M. H.; Cheng, K. C. *Acta Biomater.* **2012**, *11*, 3875.
7. Aouf, C.; Nouailhas, H.; Fache, M. *Eur. Polym. J.* **2013**, *49*, 1185.
8. Kong, Z.; Huang, H.; You, Z. *Chem. Ind. Forest Prod.* **2005**, *25*, 33.
9. Kim, H.; Abdala, A. A.; Macosko, C. W. *Macromolecules* **2010**, *43*, 6515.
10. Eigler, S.; Grimm, S.; Hof, F. *J. Mater. Chem. A* **2013**, *1*, 11559.
11. Cui, L.; Liu, J.; Wang, R. *J. Polym. Sci. Part A: Polym. Chem.* **2012**, *50*, 4423.
12. Tseng, I.; Liao, Y.; Chiang, J.; Tsai, M. *Mater. Chem. Phys.* **2012**, *136*, 247.
13. Bai, Y. Z.; Huang, H.; Kang, F. J. *Mater. Chem. A* **2013**, *1*, 9536.
14. Ryu, S. H.; Shanmugharaj, A. M. *Mater. Chem. Phys.* **2014**, *146*, 478.
15. Bora, C.; Gogoi, P.; Baglari, S.; Dolui, S. K. *J. Appl. Polym. Sci.* **2013**, *129*, 3432.
16. Bortz, D. R.; Heras, E.; Martin-Gullon, G. I. *Macromolecules* **2011**, *45*, 238.
17. Qian, X. L.; Song, B.; Yu, J. *Mater. Chem. A* **2013**, *1*, 6822.
18. Hodlur, R. M.; Rabinal, M. K. *Compos. Sci. Technol.* **2014**, *90*, 160.
19. King, J. A.; Klimek, D. R.; Miskioglu, I.; Odegard, G. M. *J. Appl. Polym. Sci.* **2013**, *128*, 4217.
20. Liu, L.; Ye, Z. *Polym. Degrad. Stab.* **2009**, *94*, 1972.
21. Munoz, J. C.; Ku, H.; Cardona, F. *J. Mater. Proc. Technol.* **2008**, *202*, 486.

22. Sturiale, A.; Vazquez, A.; Cisilino, A. *Int. J. Adhes. Adhes.* **2007**, *27*, 156.
23. Ryu, B. Y.; Emrick, T. *Macromolecules* **2011**, *44*, 5693.
24. Xu, Z.; Gao, C. *ACS Nano* **2011**, *5*, 2908.
25. Zhu, D.; Pignatello, J. *J. Environ. Sci. Technol.* **2005**, *39*, 2033.
26. Lin, D.; Xing, B. *Environ. Sci. Technol.* **2008**, *42*, 5917.
27. Gillham, J. K. *Polym. Int.* **1997**, *44*, 262.
28. Brandalise, R. N.; Zeni, M.; Martins, J. D. N.; Forte, M. M. C. *Polym. Bull.* **2009**, *62*, 33.
29. Yu, B.; Wang, X.; Xing, W. *Ind. Eng. Chem. Res.* **2012**, *51, 14*, 629.
30. Hagen, R.; Salman, L.; Stenberg, B. *J. Polym. Sci. Part B: Polym. Phys.* **1996**, *34*, 1997.
31. Murayama, T. Dynamic Mechanical Analysis of Polymeric Material; Netherland Press: 1978; Chen F-T trans, Chinese light industry press: Beijing, 1988.
32. Wang, J.; Zhan, Y.; Fang, J. *J. Appl. Polym. Sci.* **2012**, *123*, 1024.
33. Chen, Y.; Chen, Z.; Liu, H. *Acta Polym. Sinica* **2008**, *1* 399.
34. Jin, F. L.; Park, S. *J. Polym. Degrad. Stab.* **2012**, *97*, 2148.
35. Friedman, H. L. *J. Polym. Sci. Part C: Polym. Symp.* **1964**, *6*, 183.
36. Ogata, M.; Kinjo, N.; Kawata, T. *J. Appl. Polym. Sci.* **1993**, *48*, 583.
37. Zhu, W.; Wang, X.; Wang, P.; Zhang, W.; Ji, J. *J. Appl. Polym. Sci.* **2013**, *130*, 4075.
38. Zuiderduin, W. C. J.; Westzaan, C.; Huetink, J.; Gaymans, R. J. *Polymer* **2003**, *44*, 261.
39. Liu, T. I.; Phang, Y.; Shen, L. S.; Chow, Y.; Zhang, W. D. *Macromolecules* **2004**, *37*, 7214.
40. Liu, Y.; Li, Y.; Yang, Y. G. *New Carbon Mater.* **2012**, *27*, 377.
41. Cai, D.; Jin, J.; Yusoh, K. *Compos. Sci. Technol.* **2012**, *2*, 702.
42. Coleman, J. N.; Khan, U. Y.; Gun'ko, K. *Adv. Mater.* **2006**, *18*, 689.
43. Achaby, M. E.; Essamlali, Y.; Miri, N. E.; Snik, A.; Abdelouahdi, K.; Fihri, A.; Zahouily, M.; Solhy, A. *J. Appl. Polym. Sci.* **2014**, *131*, 22, DOI: 10.1002/app.41042.